A Laplace Equation on a Rectangle With Mixed Boundary Conditions

Elias Hohl[†]

Project advisor: Giovanni Felder[‡]

Abstract. We find analytical solutions of the Laplace equation on a rectangular domain with Dirichlet-Neumann boundary condition type transition occurring on a side of the rectangle. The problem can be tackled either by cutting the domain in two parts and solving the obtained coupled Laplace equations using a Fourier series approach, or by creating a conformal mapping based on Christoffel-Schwarz and Möbius transformations between the original domain and another rectangular domain where the solution of the problem is less challenging. Apart from solving for the temperature field, we also compute a coefficient, dependent only on the geometry of the domain, from which the thermal resistance of a system with the given cross-section can be computed. We conduct an experiment to confirm the validity of our model. Using our results from the Christoffel-Schwarz method, we derive regularity results for the Fourier coefficients of the coupling method. We not only determine the order of decay, but also find formulas for explicit upper bounds of the absolute value of the coefficients. These results can be used to obtain maximum error bounds for a numerical computation considering only a finite number of Fourier coefficients. Furthermore, we prove that the solutions obtained via the coupling method converge to the actual solution.

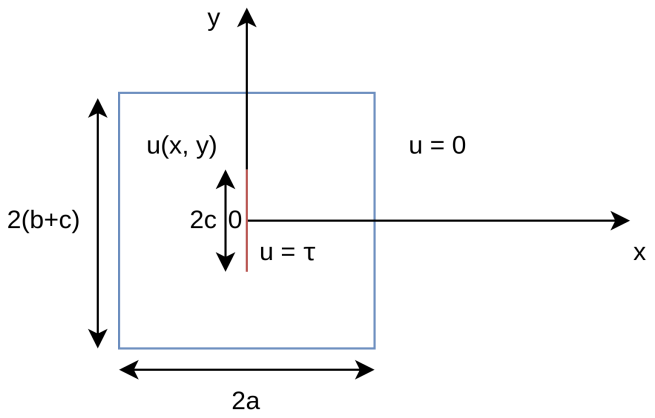

Figure 1: Sketch of the original problem.

1. Introduction. The motivation behind this study was an experimental setup (created for use in a Physics Olympiad / European Olympiad of Experimental Science problem) consisting of a thin, hot aluminium strip between two thermally insulating plates (for a more detailed description see Section 5), with a cross section as shown in Figure 1. It was of interest to

[†]Department of Physics, ETH Zurich (elhohl@ethz.ch).
[‡]Department of Mathematics, ETH Zurich

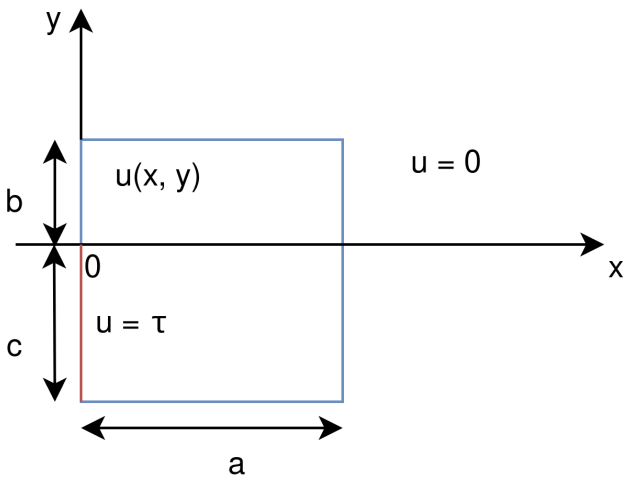

Figure 2: Sketch of the transformed problem.

analytically compute the temperature distribution $u(x, y)$ and a coefficient β quantifying the heat loss per unit height depending only on the geometry of the system (in other words, in terms of the lengths a, b, and c). Due to symmetry, it is possible to transform the problem to a rectangular domain as shown in figure Figure 2 by investigating only one quarter of the original system. Analytical solutions for the 2D Laplace equation in rectangular domains are well-known [10], also for mixed Neumann and Dirichlet boundary conditions on different sides of the rectangle [14, 15]. However, in our case, we are confronted with a mixed boundary condition on parts of the same side of the rectangle (a Dirichlet condition along c and a Neumann condition along b).

We solve the resulting problem using two different methods.

1. It is possible to separate the domain into two rectangles without a boundary condition type transition on any side by making a horizontal cut at $y = 0$. We solve the Laplace equation in both parts by separation of variables. A sequence of unknown Fourier coefficients remains as a degree of freedom for each part. These coefficients can be determined through continuity conditions along the cut, which involves an infinite system of equations relating the coefficients from both parts to each other. We approximately solve that system of equations by inverting a matrix after dropping all but a finite number of coefficients.
2. It is possible to create a conformal mapping (consisting of Christoffel-Schwarz and Möbius transformations) between the domain and another rectangle without a boundary condition type transition on any side. In the transformed domain, the Laplace equation has an easy solution. As the solutions of the Laplace equation are invariant under conformal mappings, the solution in the transformed domain can be mapped back into the original domain to obtain the solution of the original problem.

Apart from solving for the temperature field, we also compute a coefficient, dependent only on the geometry of the domain, from which the thermal resistance of a system with the given cross-section can be computed. We conduct an experiment to confirm the validity of our model.

Using our results from the Christoffel-Schwarz method, we derive regularity results for the Fourier coefficients of the coupling method. We do not only determine the order of decay, but also prove formulas for explicit upper bounds of the absolute value of the coefficients. These results can be used to obtain maximum error bounds for a numerical computation considering only a finite amount of Fourier coefficients.

The paper is organized as follows: The Fourier solution is computed in Section 2, and the Christoffel-Schwarz solution is derived in Section 3. In Section 4, the regularity results are obtained, and in Section 5, the experimental results are described and compared to theoretical calculations. Section 6 shows our conclusions.

2. Coupled Fourier series solution of the PDE. The Laplace equation will be solved separately for $y < 0$ and $y \geq 0$, with the boundary condition along the x-axis being that both the temperature and its y-derivative must be continuous (therefore these Laplace equations are referred to as coupled, as the boundary condition of each equation cannot be written down explicitly without knowing the particular solution of the other one).

We use an approach based on Fourier series to write down formulas for $u(x, y)$ for $y < 0$ and $y \geq 0$ in terms of unknown coefficients A_n and B_n. The two equations enforcing continuity and continuity of the y-derivative along the x-axis may be written down in matrix form when viewing the coefficient sequences as vectors. The solution of the system of equations (for A_n and B_n) can now be obtained by inverting a matrix.

Let $u(x, y)$ be the temperature at location (x, y). Define $u_x = \frac{\partial u}{\partial x}$, $u_y = \frac{\partial u}{\partial y}$, $u_{xx} = \frac{\partial^2 u}{\partial x^2}$ and $u_{yy} = \frac{\partial^2 u}{\partial y^2}$. The Laplace equation can be written down as

$$u_{xx} + u_{yy} = 0 \tag{2.1}$$

2.1. Coupling Laplace equations. The solution (for the setup in Figure 2) needs to fulfill the following boundary conditions:

1. $u = 0$ on the right side
2. $u = 0$ on the top side
3. $u = \tau$ along c
4. $u_x = 0$ along b
5. $u_y = 0$ along a
6. u is continuous along the x-axis
7. u_y is continuous along the x-axis

It is known that there exists a unique solution for the boundary value problem formed by these conditions and equation (2.1) which is harmonic [9] [5, pp. 92-94] [13].

It should also be explained why the continuity of u and u_y along the x-axis imply that the Laplace equation is fulfilled along the x-axis (and are thus these conditions are sufficient). The intuition behind Lemma 2.2 is the following: To be able to glue two separately obtained solutions together at $y = 0$ and reach an equilibrium, the temperature of the pieces that

are glued together must be the same (meaning u is continuous) and the heat flux out of the lower part through a certain segment of the boundary at $y = 0$ must match the heat flux into the upper part due to energy conservation (meaning u_y is continuous). However, this does not automatically ensure that the Laplace equation is also satisfied along the x-axis. An additional condition is required.

Lemma 2.1. *Let I be an interval, $x_0 \in I$ and $f : I \to \mathbb{R}$ be a continuous function which is differentiable on $I \setminus \{x_0\}$. If $\lim_{x\to x_0} f'(x)$ exists, then f is differentiable at x_0 and $f'(x_0) = \lim_{x\to x_0} f'(x)$.*

Proof. We need to show the limit

$$\lim_{x\to x_0} \frac{f(x) - f(x_0)}{x - x_0}$$

exists and compute its value. For $x > x_0$, according to the mean value theorem there exists x_m with $x_0 < x_m < x$ and

$$f'(x_m) = \frac{f(x) - f(x_0)}{x - x_0}.$$

The proof for the case $x < x_0$ proceeds analogously. Because $x \to x_0$ implies $x_m \to x_0$, the statement follows. ∎

Lemma 2.2. *Given a piecewise combination of two separately obtained solutions for the Laplace equation for $y \leq 0$ and $y \geq 0$ which are twice continuously differentiable on $(0, a) \times (-c, 0]$ and $(0, a) \times [0, b)$, respectively, and satisfy the boundary conditions 1-5, conditions 6-7 hold if and only if the Laplace equation is satisfied along the x-axis (and therefore on the whole domain).*

Proof.

⇐ This is obvious because the Laplace equation requires its solutions to be twice differentiable with respect to space in the interior of the domain.

⇒ The solutions retrieved for the separate areas $y \geq 0$ and $y \leq 0$ are real and harmonic in the interior, therefore they are also real-analytic in the interior automatically [3, p. 19]. However, the additionally given condition that the solutions are in C^2 for $y \geq 0$ and $y \leq 0$, respectively, is required such that it is also ensured they are smooth enough on the boundary $y = 0$. Then $u_{xx}(x, y)$ is continuous and in particular continuous with respect to y for the two separate regions $y \in [0, b]$, $y \in [-c, 0]$. Because $u(x, y)$ is continuous on the x-axis with respect to y, the functions $u(x, 0)$ (and their x-derivatives of arbitrary order) provided by the generally different solutions for $y \in [0, b]$ and $y \in [-c, 0]$ must match. So $u_{xx}(x, y)$ may not have a discontinuity at $y = 0$ and therefore must be continuous on the whole domain $y \in [-c, b]$. We may write

$$\lim_{y\nearrow 0} u_{xx}(x, y) = \lim_{y\searrow 0} u_{xx}(x, y) = u_{xx}(x, 0),$$

or, in combination with equation (2.1)

$$\lim_{y\nearrow 0} u_{yy}(x, y) = \lim_{y\searrow 0} u_{yy}(x, y) = \lim_{y\to 0} u_{yy}(x, y) = -u_{xx}(x, 0).$$

Applying Lemma 2.1 for the continuous function u_y in dependence of y (while keeping x constant), it follows that

$$u_{yy}(x, 0) = -u_{xx}(x, 0),$$

which is the Laplace equation at $y = 0$ as desired. ∎

2.2. Separation of variables. Using separation of variables, the following formulas are found [10] to satisfy all boundary conditions for arbitrary coefficients A_n, B_n apart from the conditions of continuity and continuity of the y-derivative on the common boundary. For $y \geq 0$:

$$u(x,y) = \sum_{n=0}^{\infty} A_n \cos\left(\pi\left(n+\frac{1}{2}\right)\frac{x}{a}\right)\sinh\left(\frac{\pi\left(n+\frac{1}{2}\right)(y-b)}{a}\right). \tag{2.2}$$

For $y < 0$:

$$u(x,y) = -\tau\frac{x-a}{a} + \sum_{n=1}^{\infty} B_n \sin\left(\frac{\pi n x}{a}\right)\cosh\left(\frac{\pi n(y+c)}{a}\right). \tag{2.3}$$

2.3. Continuity conditions. We find that the conditions of continuity and continuity of the y-derivative hold if and only if

$$B_m^* = -\frac{8}{\pi}\coth\left(\frac{\pi m c}{a}\right)\sum_{n=0}^{\infty}\frac{A_n^*\left(n+\frac{1}{2}\right)}{(2n+1)^2-4m^2}, \tag{2.4}$$

as well as

$$A_m^* = -\frac{8}{\pi}\coth\left(\frac{\pi\left(m+\frac{1}{2}\right)b}{a}\right)\left(\frac{1}{\pi(2m+1)^2} - \sum_{n=1}^{\infty}\frac{B_n^* n}{(2m+1)^2-4n^2}\right), \tag{2.5}$$

where

$$A_m^* = \frac{A_m}{\tau}\cosh\left(\frac{\pi\left(m+\frac{1}{2}\right)b}{a}\right), \tag{2.6}$$

$$B_m^* = \frac{B_m}{\tau}\cosh\left(\frac{\pi m c}{a}\right). \tag{2.7}$$

We obtain this result by imposing the two conditions (2.8) and (2.9):

$$\begin{aligned} 0 = &\sum_{n=0}^{\infty} A_n \cos\left(\pi\left(n+\frac{1}{2}\right)\frac{x}{a}\right)\sinh\left(\frac{\pi\left(n+\frac{1}{2}\right)b}{a}\right) - \\ &\tau\frac{x-a}{a} + \sum_{n=1}^{\infty} B_n \sin\left(\frac{\pi n x}{a}\right)\cosh\left(\frac{\pi n c}{a}\right), \end{aligned} \tag{2.8}$$

$$\begin{aligned} 0 = &-\sum_{n=0}^{\infty} A_n\left(n+\frac{1}{2}\right)\cos\left(\pi\left(n+\frac{1}{2}\right)\frac{x}{a}\right)\cosh\left(\frac{\pi\left(n+\frac{1}{2}\right)b}{a}\right) + \\ &\sum_{n=1}^{\infty} B_n n \sin\left(\frac{\pi n x}{a}\right)\sinh\left(\frac{\pi n c}{a}\right). \end{aligned} \tag{2.9}$$

To solve the problem, one needs to find the value of the coefficients A_n, B_n such that equations (2.8) and (2.9) are fulfilled for all $x \in [0, a]$. This system of equations can be rewritten

using (generalized) Fourier series, due to the orthogonality properties of sine and cosine. Let $m, n \in \mathbb{N}$:

$$\int_0^a \sin\left(\frac{\pi n x}{a}\right) \sin\left(\frac{\pi m x}{a}\right) dx = \begin{cases} \frac{a}{2} & \text{if } m = n \\ 0 & \text{if } m \neq n, \end{cases} \tag{2.10}$$

$$\int_0^a \cos\left(\frac{\pi \left(n + \frac{1}{2}\right) x}{a}\right) \cos\left(\frac{\pi \left(m + \frac{1}{2}\right) x}{a}\right) dx = \begin{cases} \frac{a}{2} & \text{if } m = n \\ 0 & \text{if } m \neq n. \end{cases} \tag{2.11}$$

Applying the orthogonality property (2.11) to equation (2.8), and equivalently applying (2.10) to (2.9), we obtain (2.5) and (2.4), as desired.

To find a solution, equation (2.4) is written in matrix form after replacing ∞ with a large number $N-1$ to find an approximate solution. The convergence of this method will be proven in Subsection 4.2. The resulting matrix equations are

$$\vec{B}^* = M_1 \vec{A}^*, \tag{2.12}$$

$$\vec{A}^* = M_2 \vec{B}^* = M^{-1} \vec{v}, \tag{2.13}$$

where $\vec{A}^*, \vec{B}^* \in \mathbb{R}^N$ and $M_1 \in \mathrm{Mat}_{N\times N}(\mathbb{R})$ and

$$M_{1,ij} := \begin{cases} -\frac{8}{\pi} \coth\left(\frac{\pi i c}{a}\right) \frac{\left(j + \frac{1}{2}\right)}{(2j+1)^2 - 4i^2} & \text{if } i > 0 \\ 0 & \text{if } i = 0, \end{cases} \tag{2.14}$$

$$M_2 = \left(\frac{8}{\pi} \frac{j}{(2i+1)^2 - 4j^2} \coth\left(\frac{\pi \left(i + \frac{1}{2}\right) b}{a}\right)\right) \in \mathrm{Mat}_{N\times N}(\mathbb{R}), \tag{2.15}$$

$$\vec{v} = \left(\frac{8}{\pi^2 (2i+1)^2} \coth\left(\frac{\pi \left(i + \frac{1}{2}\right) b}{a}\right)\right) \in \mathbb{R}^N, \tag{2.16}$$

$$M = M_2 M_1 - I. \tag{2.17}$$

The closed form expression for M is

$$M_{ik} = -\delta_{ik} - \frac{64}{\pi^2} \sum_{j=1}^{N-1} \frac{j \left(k + \frac{1}{2}\right) \coth\left(\frac{\pi\left(i+\frac{1}{2}\right)b}{a}\right) \coth\left(\frac{\pi j c}{a}\right)}{\left((2i+1)^2 - 4j^2\right)\left((2k+1)^2 - 4j^2\right)}. \tag{2.18}$$

Lemma 2.3. *The matrix $M \in Mat_{N\times N}(\mathbb{R})$ as defined by equation (2.18) using an arbitrary $N \geq 2$ is invertible for all possible parameter values $a, b, c \in \mathbb{R}_{>0}$.*

Proof. We may decompose the matrix as $M = -D^{-1}(I + S)D$ where D and S are a diagonal and a symmetric matrix, respectively, defined by

$$D_{ii} = \sqrt{\frac{2i+1}{2\coth\left(\pi\left(i + \frac{1}{2}\right)\frac{b}{a}\right)}},$$

$$S_{ik} = \sum_{j=1}^{N-1} d_j C_{ji} C_{jk},$$

where

$$d_j = \frac{64}{\pi^2} j \coth\left(\frac{\pi j c}{a}\right),$$

$$C_{ji} = \frac{1}{(2i+1)^2 - 4j^2} \sqrt{\left(i+\frac{1}{2}\right) \coth\left(\pi\left(i+\frac{1}{2}\right)\frac{b}{a}\right)}.$$

For an arbitrary vector $z \in \mathbb{R}^N$,

$$z^T S z = \sum_{i=0}^{N-1}\sum_{k=0}^{N-1}\sum_{j=1}^{N-1} d_j C_{ji} C_{ki} z_i z_k = \sum_{j=1}^{N-1} d_j \left(\sum_{i=0}^{N-1} C_{ji} z_i\right)^2 \geq 0.$$

Therefore, S is positive semi-definite. As I is a positive definite matrix, $I + S$ is positive definite and thus invertible, which implies M is invertible. ∎

Figure 3 shows the temperature field given by equations (2.3) and (2.2) with coefficients determined by exact numerical inversion of the matrix defined by (2.18) (using $N = 100$) after transforming the problem back to the original statement shown in Figure 1.

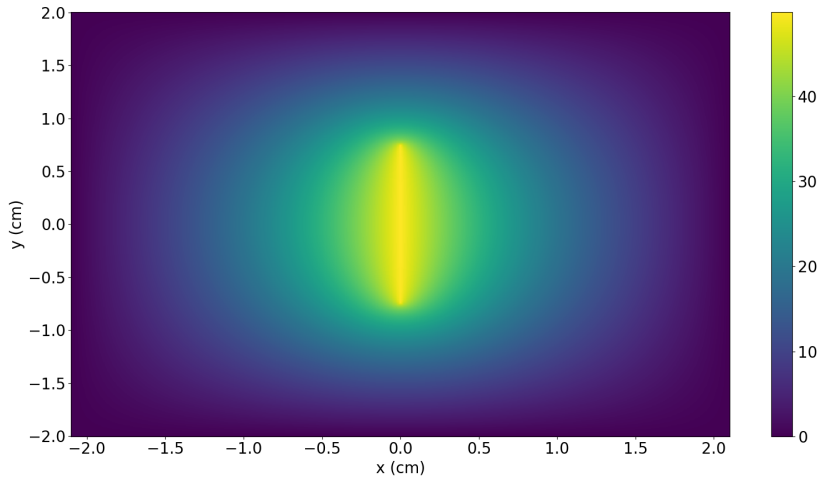

Figure 3: Temperature field derived by matrix inversion ($a = 2.1cm$, $b = 1.25cm$, $c = 0.75cm$, $\tau = 50K$, $N = 100$).

2.4. Heat flux. We want to compute a coefficient β depending only on the geometry of the setup and quantifying the heat flux ΔP through the heated side (parallel to the yz-plane and containing the line c) in a setup as shown in Figure 2 extended to a height Δz along the z-axis. Define

$$\vec{w} = \left(\tanh\left(\frac{\pi i c}{a}\right)\right) \in \mathbb{R}^N, \tag{2.19}$$

and

$$\beta = \frac{\Delta P}{\lambda \tau \Delta z}, \tag{2.20}$$

where λ is the thermal conductivity. We claim that equation (2.21) holds, where $\langle \cdot, \cdot \rangle$ is the standard scalar product.

$$\beta = \frac{c}{a} - \langle M_1 M^{-1} \vec{v}, \vec{w} \rangle. \tag{2.21}$$

The heat flux through the area dA can be computed by

$$\Delta P = \frac{\partial Q}{\partial t} = -\lambda \int dy \Delta z u_x(0, y), \tag{2.22}$$

where

$$u_x = \frac{\partial u}{\partial x} = -\frac{\tau}{a} + \frac{\pi}{a} \sum_{n=1}^{\infty} B_n n \cos\left(\frac{\pi n x}{a}\right) \cosh\left(\frac{\pi n (y+c)}{a}\right). \tag{2.23}$$

Therefore,

$$\begin{aligned} \Delta P &= -\lambda \Delta z \int_{-c}^{0} \left(-\frac{\tau}{a} + \frac{\pi}{a} \sum_{n=1}^{\infty} B_n n \cosh\left(\frac{\pi n (y+c)}{a}\right) \right) dy \\ &= \frac{\lambda \Delta z}{a} \left(\tau c - a \sum_{n=1}^{\infty} B_n \sinh\left(\frac{\pi n c}{a}\right) \right). \end{aligned} \tag{2.24}$$

Combining equations (2.19), (2.24), (2.12), (2.20) and (2.7), equation (2.21) follows.

3. Christoffel-Schwarz solution of the PDE. Using the Christoffel-Schwarz mapping, we can transform the problem from Figure 2 to a simpler domain where it is easier to find the solution. The idea is the following:

1. Shift the rectangle from Figure 2 so that the bottom side lies on the horizontal axis and it is centered around the vertical axis. Scale it appropriately and transform it into the upper half plane with vertices $-1/k$, -1, 1, $1/k$ where $0 < k < 1$ using the inverse of the Christoffel-Schwarz mapping. The point on the left edge of the rectangle where the boundary condition changes gets mapped to $-1/m$ in the upper half plane, where $k < m < 1$.
2. Map the quadruple of points $-1/k$, $-1/m$, -1, 1 to $-1/l$, -1, 1, $1/l$ where $0 < l < 1$ using a Möbius transformation. It must be assured that the line segments between each pair of points also gets mapped to the correct corresponding line segment in the transformed domain to preserve the order of boundary conditions. Note that the point $-1/k$ gets mapped to some unknown place right of $1/l$, but this does not matter as the boundary condition does not change at this vertix.
3. Map the quadruple of points $-1/l$, -1, 1, $1/l$ to another rectangle in the upper half plane.
4. Solve the Laplace equation in the new rectangle (which is extremely easy, we will show that the solution in this domain is an affine linear function).

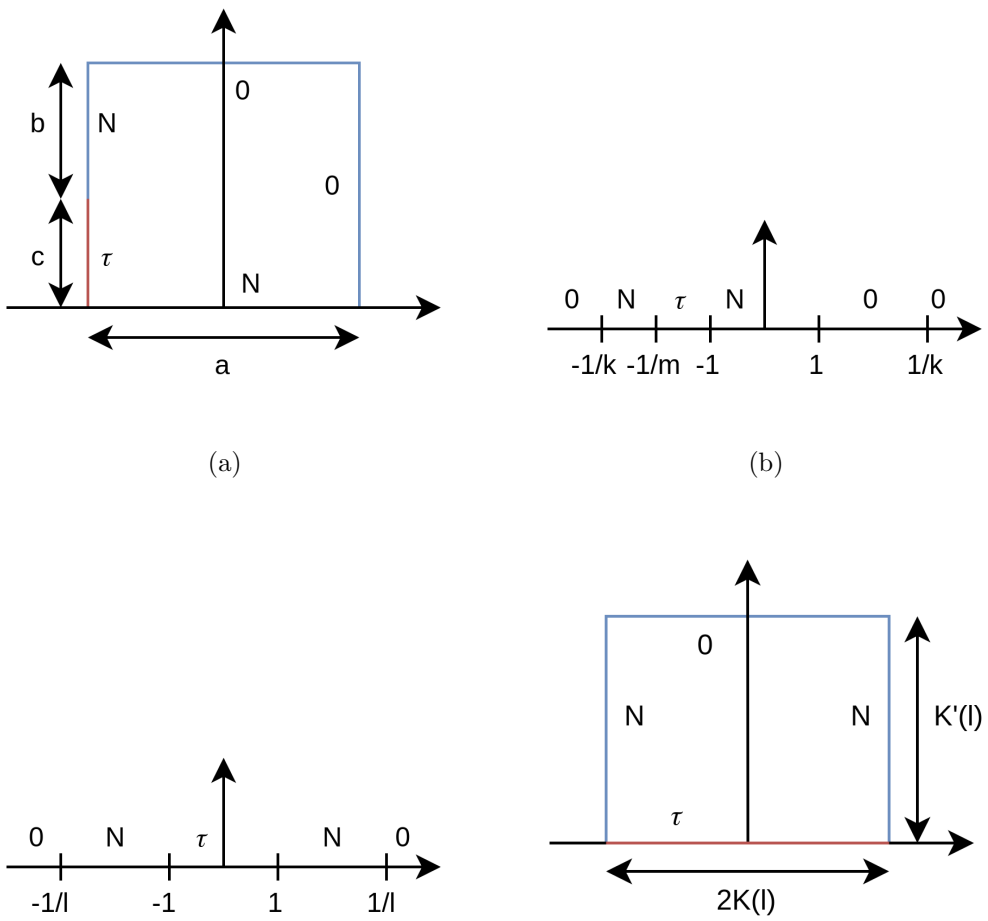

(a) (b)

(c) (d)

Figure 4: Idea for the Christoffel-Schwarz solution method: The original domain is shown in (a), which is mapped to the upper half plane (b) using an inverse Christoffel-Schwarz transformation; a Möbius transformation is used to reposition the vertices in the upper half plane (c), and after applying a Christoffel-Schwarz transformation, we receive rectangle (d). Here, 0 and τ denote Dirichlet boundary conditions (the temperature is 0 or τ, respectively). N denotes a Neumann boundary condition (the derivative of the temperature is 0).

3.1. Inverse Christoffel-Schwarz transformation. To determine the correct scaling factor, we need to solve the system of equations (3.1), (3.2)

$$a = 2\alpha K(k), \tag{3.1}$$

$$b + c = \alpha K'(k), \tag{3.2}$$

where K is the complete elliptic integral of the first kind, and $K'(k) = K(\sqrt{1-k^2})$. This gives an expression which allows k to be determined from the given half-period ratio

$$\frac{\omega_2}{\omega_1} = i\frac{K'(k)}{K(k)} = i\frac{b+c}{2a}. \tag{3.3}$$

We also get

$$\alpha = \frac{2}{aK(k)}. \tag{3.4}$$

The inverse of the Christoffel-Schwarz mapping from the scaled rectangle with vertices $-a/(2\alpha)+i(b+c)/\alpha$, $-a/(2\alpha)$, $a/(2\alpha)$, $a/(2\alpha)+i(b+c)/\alpha$ to the upper half plane with the vertices being mapped to $-1/k$, -1, 1, $1/k$ is the Jacobi elliptic function $\mathrm{sn}(z,k)$. [8]

3.2. Möbius transformation.

Lemma 3.1. *Let z_1, z_2, z_3, z_4 be a quadruple of distinct points on the real axis with $z_1 < z_2 < z_3 < z_4$. There exists a unique Möbius transformation which maps this quadruple to $-1/l$, -1, 1, $1/l$ where $0 < l < 1$.*

Proof. Define the cross-ratio as

$$(z_1, z_2; z_3, z_4) = \frac{z_1 - z_3}{z_2 - z_3} \cdot \frac{z_2 - z_4}{z_1 - z_4}.$$

The map

$$h(z) = \frac{z_1 - z_3}{z_2 - z_3} \cdot \frac{z_2 - z}{z_1 - z}$$

sends z_1 to ∞, z_2 to 0, z_3 to 1, and z_4 to $(z_1, z_2; z_3, z_4)$. Therefore, two quadruples of points with the same cross-ratio can be mapped to each other with a Möbius map. The converse is also true, because cross-ratio is preserved by $z \mapsto az$, $z \mapsto z + b$, and $z \mapsto \frac{1}{z}$, which generate all Möbius transformations. It remains to find the quadruples $1, -1; 1/l, -1/l$ with given cross-ratio. Define

$$r = (z_3, z_2; z_4, z_1) = \frac{z_3 - z_4}{z_2 - z_4} \cdot \frac{z_2 - z_1}{z_3 - z_1}.$$

Due to the given order of z_i, we have $0 < r < 1$. For a Möbius transformation to exist, it is needed that

$$r = (1, -1; 1/l, -1/l) = \frac{1 - 1/l}{-1 - 1/l} \cdot \frac{-1 + 1/l}{1 + 1/l} = \left(\frac{1-l}{1+l}\right)^2.$$

The solutions of this equation are

$$l = \frac{1 - \sqrt{r}}{1 + \sqrt{r}}$$

and its reciprocal. [16] As $0 < l < 1$, the former is the correct (and unique) solution. ∎

Lemma 3.2. *Let $M(z) = (Az + B)/(Cz + D)$ be a Möbius transform which maps the triple of real points (z_1, z_2, z_3) to another triple of real points (w_1, w_2, w_3). Then A, B, C and D can be chosen to be real.*

Proof. According to the proof of Lemma 3.1, two points can be matched to each other if the cross-ratios match:

$$\frac{(z - z_3)(z_1 - z_2)}{(z - z_3)(z_1 - z_3)} = \frac{(w - w_3)(w_1 - w_2)}{(w - w_3)(w_1 - w_3)}.$$

This yields

$$M(z) = w = \frac{w_2(w_1 - w_3)(z - z_3)(z_1 - z_2) - w_3(w_1 - w_2)(z - z_2)(z_1 - z_3)}{(w_1 - w_2)(z - z_2)(z_1 - z_3) - (w_1 - w_3)(z - z_3)(z_1 - z_2)},$$

which is a Möbius transformation of the given form, with real values of A, B, C and D. ∎

Lemma 3.3. *Let $M(z) = (Az + B)/(Cz + D)$ be a Möbius transform, where A, B, C and D are real. If $AD - BC > 0$, then M maps the upper half plane to the upper half plane.*

Proof.

$$\operatorname{Im} M(z) = \operatorname{Im} \frac{(Az + B)(C\overline{z} + D)}{|Cz + D|^2} = \operatorname{Im} \frac{ADz + BC\overline{z}}{|Cz + D|^2} = \frac{AD - BC}{|Cz + D|^2} \operatorname{Im} z.$$

For $z \in \mathbb{H}$, this is positive if and only if $AD - BC > 0$. Therefore, $M(\mathbb{H}) \subseteq \mathbb{H}$. As taking the inverse of M does not change the sign of $AD - BC$, we can also state $M^{-1}(\mathbb{H}) \subseteq \mathbb{H}$. Together, this implies $M(\mathbb{H}) = \mathbb{H}$. ∎

Lemma 3.4. *Let $\mathbb{C}^* = \mathbb{C} \cup \tilde{\infty}$ be the extended complex plane and $\mathbb{R}^* = \mathbb{R} \cup \tilde{\infty}$ ($\tilde{\infty}$ denotes complex infinity). There exist a unique Möbius transformation $M : \mathbb{C}^* \to \mathbb{C}^*$ and a unique real number l which fulfill the following conditions:*

1. $M(-1/k) = -1/l$, $M(-1/m) = -1$, $M(-1) = 1$, $M(1) = 1/l$
2. $M(\mathbb{R}^*) = \mathbb{R}^*$
3. $0 < l < 1$
4. $M([-1/k, -1/m]) = [-1/l, -1]$, $M([-1/m, -1]) = [-1, 1]$, $M([-1, 1]) = [1, 1/l]$.

Proof. The first and third conditions are satisfied due to Lemma 3.1. The fourth condition follows as a consequence of the first and second conditions: If the inversion ($M(z_{inv}) = \infty$) happens for some $z_{inv} \in [-1/k, 1]$, the order of the vertices also cannot be preserved, which contradicts the first condition. It remains to be shown that M maps the upper half plane to the upper half plane and the extended real axis to the extended real axis. The latter follows directly from Lemma 3.2, which states that the Möbius transform M is real. This implies that also the first condition of Lemma 3.3 is satisfied. Now we need to differentiate between two cases. Let $M(z) = (Az + B)/(Cz + D)$. If $C = 0$, then M is a linear function with real parameters. $AD = AD - BC$ must be positive, because the four points on the real axis are mapped by M in an order-preserving way. This concludes the proof for $C = 0$. If $C \neq 0$, we can normalize the map to $C = 1$ without changing it. Solving the system of equations $M(-1/k) = -1/l$, $M(-1) = 1$, $M(1) = 1/l$, we get

$$A = \frac{3lk - l + k + 1}{l(lk + l + 3k - 1)}$$

$$B = \frac{-lk + 3l + k + 1}{l(lk + l + 3k - 1)}$$

$$D = \frac{lk + l - k + 3}{lk + l + 3k - 1}$$

$$AD - BC = \frac{4(1 - k^2)(1 - l^2)}{l\,(kl + 3k + l - 1)^2}.$$

Therefore, $AD - BC > 0$ also for $C \neq 0$. ∎

Lemma 3.4 proves the existence and uniqueness of the desired Möbius transformation for all possible parameter values a, b, c. We can compute an explicit expression by solving the system of equations given in the theorem. Plugging in the expressions for A, B, D already computed as a part of its proof into the remaining equation $M(-1/m) = -1$ yields

$$\frac{-3lk + l - k + m\,(-lk + 3l + k + 1) - 1}{l\,(-lk - l - 3k + m\,(lk + l - k + 3) + 1)} = -1, \tag{3.5}$$

which can be reformulated as a quadratic equation with the solutions

$$l = \frac{km + 3k - 3m - 2\sqrt{2}\sqrt{(1-k)(m-k)(m+1)} - 1}{(k+1)(m-1)}, \tag{3.6}$$

$$l = \frac{km + 3k - 3m + 2\sqrt{2}\sqrt{(1-k)(m-k)(m+1)} - 1}{(k+1)(m-1)}, \tag{3.7}$$

under the assumption that the denominator in (3.5) is not zero when l is one of the given solutions. This assumption is true: If, for any x, the equation

$$\frac{Ax + B}{Cx + D} = -1 \tag{3.8}$$

holds, and the denominator $Cx+D$ equals zero, (3.8) may be rewritten as $Ax+B = Cx+D = 0$, which is impossible to be satisfied as $AD - BC > 0$.

The given solutions for l are reciprocals of each other, therefore, one of them is the correct solution $0 < l < 1$, and the other one is greater than 1. The denominator is always negative as $m < 1$. This means the second solution is the smaller and thus the correct one.

3.3. Christoffel-Schwarz transformation. The Christoffel-Schwarz mapping from the upper half plane with vertices $-1/l$, -1, 1, $1/l$ to a rectangle located in the upper half plane (with the bottom side on the real axis and horizontally centered around the imaginary axis) is given by an incomplete elliptic integral of the first kind [2, p. 589]

$$f(z, l) = \int_0^z \frac{dt}{\sqrt{1 - t^2}\sqrt{1 - l^2 t^2}}. \tag{3.9}$$

The horizontal and vertical side lengths of the rectangle are again $2K(l)$ and $K'(l)$, respectively. [8]

3.4. Solution in the transformed rectangle. In the transformed rectangle, the boundary conditions are:

1. A Neumann condition $\partial u/\partial x = 0$ along both vertical sides
2. A Dirichlet condition $u = \tau$ along the bottom side
3. A Dirichlet condition $u = 0$ along the top side

The solution in this domain is simply given by

$$u(w) = \tau \left(1 - \frac{\operatorname{Im} w}{K'(l)}\right). \tag{3.10}$$

Expressing this in terms of the coordinate $z = x + iy$ in the original domain, we get

$$u(z) = \tau \left(1 - \frac{1}{K'(l)} \operatorname{Im} f\left(\frac{A\operatorname{sn}(z/\alpha, k) + B}{\operatorname{sn}(z/\alpha, k) + D}, l\right)\right). \tag{3.11}$$

The result looks visually the same as when derived using the Fourier method (Figure 3).

3.5. Heat flux. Equation (3.11) allows to compute expressions for the heat flux and thermal resistance. Applying (2.22), we get

$$\begin{aligned}\Delta P &= -\lambda \Delta z \int_0^c u_x(-a/2+iy)dy \\ &= \frac{\lambda \Delta z \tau}{K'(l)} \int_0^c \frac{\partial}{\partial x} \operatorname{Im} f\left(\frac{A\operatorname{sn}((-a/2+iy)/\alpha,k)+B}{\operatorname{sn}((-a/2+iy)/\alpha,k)+D}, l\right) dy \\ &= -\frac{\lambda \Delta z \tau}{K'(l)} \int_0^c \frac{\partial}{\partial y} \operatorname{Re} f\left(\frac{A\operatorname{sn}((-a/2+iy)/\alpha,k)+B}{\operatorname{sn}((-a/2+iy)/\alpha,k)+D}, l\right) dy \\ &= \frac{\lambda \Delta z \tau}{K'(l)} \left(\operatorname{Re} f\,(1,l) - \operatorname{Re} f\,(-1,l)\right) \\ &= \frac{2\lambda \Delta z \tau K(l)}{K'(l)}.\end{aligned} \tag{3.12}$$

Here we have used the second Cauchy-Riemann equation to express the x-derivative in terms of an y-derivative. Note that this result shows that the heat flux in the original and transformed domain are equal. Using (2.20), an explicit expression for β can also be computed:

$$\beta = \frac{2K(l)}{K'(l)}. \tag{3.13}$$

4. Regularity results.

4.1. Fourier coefficient bounds. The goal of this section is to find upper bounds for the coefficients A_n in equation (2.2) (the same can be done for the coefficients B_n in equation (2.3), the computation is similar).

Note that we will use the complex notation $u(z)$ for the temperature field as defined in Section 3. First of all, define the interior domain of the untransformed rectangle in the complex plane to be

$$\Omega = \left\{ z \in \mathbb{C} \,|\, 0 < \operatorname{Im}(z) < b+c, -\frac{a}{2} < \operatorname{Re}(z) < \frac{a}{2} \right\}, \tag{4.1}$$

and the z_0-shifted domain as

$$\Omega_0 = \Omega - z_0. \tag{4.2}$$

Furthermore, define

$$\hat{A}_n = -A_n \sinh\left(\frac{\pi\left(n+\frac{1}{2}\right)b}{a}\right) \tag{4.3}$$

to express the temperature along the horizontal line which interesects the point of boundary condition change as

$$u(x+z_0) = \sum_{n=0}^{\infty} \hat{A}_n \cos\left(\pi\left(n+\frac{1}{2}\right)\frac{x}{a}\right), \tag{4.4}$$

where $z_0 = -a/2 + ic$. The coefficients $\hat{A}_n$ are given by

$$\begin{aligned}\hat{A}_n &= \frac{2}{a}\int_0^a u(x+z_0)\cos\left(\pi\left(n+\frac{1}{2}\right)\frac{x}{a}\right)dx \\ &= -\frac{4}{\pi(2n+1)}\int_0^a u_x(x+z_0)\sin\left(\pi\left(n+\frac{1}{2}\right)\frac{x}{a}\right)dx \\ &= \frac{4\tau}{K'(l)\pi(2n+1)}\operatorname{Im}\int_0^a \frac{v(x)}{\sqrt{x}}\sin\left(\pi\left(n+\frac{1}{2}\right)\frac{x}{a}\right)dx\end{aligned} \tag{4.5}$$

after applying integration by parts, plugging in expression (3.11) and defining

$$v(x) = \frac{g'(x+z_0)\sqrt{x}}{\sqrt{1-g^2(x+z_0)}\sqrt{1-l^2g^2(x+z_0)}} \tag{4.6}$$

and

$$g(z) = M(\operatorname{sn}(z,k)) = \frac{A\operatorname{sn}(z/\alpha,k)+B}{\operatorname{sn}(z/\alpha,k)+D}. \tag{4.7}$$

Lemma 4.1. *There exists an open set Ω_0' containing the line segment $\overline{\Omega_0}\cap\mathbb{R}$ such that $v(x)$ is holomorphic on Ω_0'.*

Proof. We will construct the open set as $\Omega_0' = \Omega_0 \cup B_\epsilon(0) \cup B_\epsilon(a)$. It is obvious that $v(x)$ is holomorphic on Ω_0 because the Christoffel-Schwarz and Möbius transformations are per definition holomorphic in the interior of the domain, and $\sqrt{x}$ has a holomorphic extension on the complex plane with a branch cut along the negative real axis. It remains to be shown that $v(x)$ is holomorphic on $B_\epsilon(0)$ and $B_\epsilon(a)$.

To investigate the behavior at $x = 0$, write

$$v(x) = \frac{\sqrt{x}}{\sqrt{g(x+z_0)+1}}q(x) = \left(\frac{g(x+z_0)-g(z_0)}{x}\right)^{-1/2}q(x),$$

where

$$q(x) = \frac{g'(x+z_0)}{\sqrt{1-g(x+z_0)}\sqrt{1-lg(x+z_0)}\sqrt{1+lg(x+z_0)}}$$

is holomorphic in a neighbourhood $B_\epsilon(0)$, as its singularities correspond to the vertices of the rectangle that are not located at $x = 0$ or otherwise $\operatorname{sn}(z/\alpha,k) + D = 0$, which is the inversion point of the Möbius transformation that must be somewhere on the upper or right side of the (untransformed) rectangle (the Jacobi elliptic sine is not necessarily injective on the extended domain Ω_0', but the above reasoning shows that $\operatorname{sn}(z_0/\alpha,k) \neq -D$, and we can use the continuity of the Jacobi elliptic sine at z_0 to shrink ϵ until $-D \notin \operatorname{sn}(B_\epsilon(0)/\alpha,k)$). $g(z)$ does not have other non-removable singularities, as the Jacobi elliptic sine is meromorphic and therefore $g(z) \to A$ at its singularities. Define

$$p(x) = \frac{g(x+z_0)-g(z_0)}{x},$$

which can be extended holomorphically by setting $p(0) = g'(z_0)$ (using the Riemann extension theorem). Note that $0 \notin p(B_\epsilon(0))$ because

$$\begin{aligned}g'(z) &= \frac{AD-B}{\alpha\left(\operatorname{sn}(z/\alpha,k)+D\right)^2}\operatorname{cn}(z/\alpha,k)\operatorname{dn}(z/\alpha,k) \\ &= \frac{AD-B}{\alpha\left(\operatorname{sn}(z/\alpha,k)+D\right)^2}\sqrt{1-\operatorname{sn}^2(z/\alpha,k)}\sqrt{1-k^2\operatorname{sn}^2(z/\alpha,k)},\end{aligned}$$

which cannot be zero as $AD-B>0$ according to Lemma 3.4, and the Jacobi elliptic cosine and delta function are only zero at the vertices of the (untransformed) rectangle (another continuity argument can be used to resolve issues with non-injectivity on the extended domain). Then $v(x)=q(x)/\sqrt{p(x)}$ is holomorphic on $B_\epsilon(0)$.

At $x=a$, the denominator of $v(x)$ cannot have a zero as z_0+a is not a special point coinciding with any of the vertices of the transformed rectangle. However, we need to show that $g'(x+z_0)$ does not have a singularity at $x=a$. Define $h(z)=1/g(z)$, which is possible as $g(z)$ is nonzero in a neighbourhood of z_0+a (the zero of $g(z)$ lies on the left, hot side of the untransformed rectangle; another continuity argument can be used to resolve issues with non-injectivity on the extended domain). We can write

$$g'(x+z_0)=\frac{-h'(x+z_0)}{h^2(x+z_0)},$$

and

$$\begin{aligned}h'(z)&=-\frac{AD-B}{\alpha\left(A\mathrm{sn}(z/\alpha,k)+B\right)^2}\mathrm{cn}(z/\alpha,k)\mathrm{dn}(z/\alpha,k)\\&=-\frac{AD-B}{\alpha\left(A\mathrm{sn}(z/\alpha,k)+B\right)^2}\sqrt{1-\mathrm{sn}^2(z/\alpha,k)}\sqrt{1-k^2\mathrm{sn}^2(z/\alpha,k)}.\end{aligned}$$

$\mathrm{sn}(z/\alpha,k)$ has no singularities in a neighbourhood of z_0+a, as the only singular point in $\overline{\Omega}$ is at the center of the upper boundary of the (untransformed) rectangle. $A\mathrm{sn}(z/\alpha,k)+B\neq 0$ in a neighbourhood of z_0+a: This follows from $0\notin g(B_\epsilon(z_0+a))$, which was proved above. $A\mathrm{sn}(z/\alpha,k)+B=0$ for a given value of z necessarily implies $g(z)=0$, as its numerator is 0 and the denominator cannot also be 0 (otherwise, $AD-B=0$ which is a contradiction to M being a well-defined Möbius transformation). We can conclude that $h'(z)$ is holomorphic on $B_\epsilon(z_0+a)$. We may write

$$v(x)=\frac{-h'(x+z_0)\sqrt{x}}{\sqrt{h^2(x+z_0)-1}\sqrt{h^2(x+z_0)-l^2}}.$$

The denominator of the above expression is nonzero when x in a neighbourhood of a, as $\lim_{x\to a}h(x+z_0)\notin\{1,-1,l,-l\}$. This follows from the previously stated fact that $\lim_{x\to a}g(x+z_0)\notin\{1,-1,1/l,-1/l\}$. The square root has a holomorphic extension in the investigated neighbourhood, as $a\neq 0$. It follows that $v(x)$ is holomorphic on $B_\epsilon(a)$. This concludes the proof. ∎

We can expand (4.5) to

$$\hat{A}_n=\frac{4\tau}{K'(l)\pi(2n+1)}\left(\mathrm{Im}\,I_1+\mathrm{Im}\,I_2\right), \tag{4.8}$$

where we define

$$I_1=\int_0^a\frac{v(0)}{\sqrt{x}}\sin\left(\pi\left(n+\frac{1}{2}\right)\frac{x}{a}\right)dx, \tag{4.9}$$

and

$$I_2=\int_0^a\frac{v(x)-v(0)}{x}\sqrt{x}\sin\left(\pi\left(n+\frac{1}{2}\right)\frac{x}{a}\right)dx. \tag{4.10}$$

I_1 can be expressed in terms of a Fresnel integral by using the substitution $x = at^2/(2n+1)$, which yields

$$I_1 = v(0)\sqrt{\frac{4a}{2n+1}}S(\sqrt{2n+1}). \tag{4.11}$$

Lemma 4.2. *The Fresnel integral $S(x) = \int_0^x \sin\left(\frac{\pi}{2}t^2\right)dt$ is nonnegative for nonnegative real x, converges as $x \to \infty$, and the sequence of local maxima is decreasing monotonously.*

Proof. Using the substitution $z = t^2$, the Fresnel sine integral may be rewritten as

$$S(x) = \frac{1}{2}\int_0^{x^2} \frac{\sin\left(\frac{\pi}{2}z\right)}{\sqrt{z}}dz.$$

The integral may be split up at the roots of the sine in the numerator ($z = 2n$ where $n \in \mathbb{N}$). These points correspond to the local extrema of $S(x)$, as the sign changes of the integrand occur here. Due to the periodicity of the sine, the absolute value of the numerator behaves like the same function in all these intervals. As the denominator is increasing with z in a strictly monotonous way, the sequence of the absolute integral values on each interval is decreasing in a strictly monotonous way. Using the Leibniz criterion, we can conclude that $\lim_{x\to\infty} S(x)$ converges. The integral is always nonnegative, as the sine is nonnegative on the first interval. ∎

As a corollary of Lemma 4.2, the global maximum of $|S(x)|$ is the value of the first local maximum, which is $S_{max} \approx 0.713972$ [2, p. 329]. This result gives us a simplified upper bound for $|I_1|$:

$$|I_1| \leq |v(0)|\sqrt{\frac{4a}{2n+1}}S_{max}. \tag{4.12}$$

We utilize integration by parts to evaluate I_2,

$$I_2 = \frac{2a}{\pi(2n+1)}\int_0^a w'(x)\cos\left(\pi\left(n+\frac{1}{2}\right)\frac{x}{a}\right)dx, \tag{4.13}$$

where

$$w(x) = \frac{v(x)-v(0)}{\sqrt{x}}. \tag{4.14}$$

Note that the derivative $w'(x)$ is well-defined and bounded for $x \in [0, a]$ due to Lemma 4.1. We may express it as

$$w'(x) = \frac{v'(x)}{\sqrt{x}} - \frac{1}{2\sqrt{x}}\frac{v(x)-v(0)}{x}. \tag{4.15}$$

Plugging (4.15) into (4.13) and taking the absolute value to find an upper bound for I_2, we obtain

$$|I_2| \leq \frac{2a}{\pi(2n+1)}\int_0^a \left|\frac{v'(x)}{\sqrt{x}} - \frac{1}{2\sqrt{x}}\frac{v(x)-v(0)}{x}\right|dx, \tag{4.16}$$

which can be further approximated to

$$\begin{aligned} |I_2| &\leq \frac{3a}{\pi(2n+1)}\sup\left|v'(x)\right|\int_0^a \left|\frac{1}{\sqrt{x}}\right|dx \\ &= \frac{6a\sqrt{a}}{\pi(2n+1)}\sup\left|v'(x)\right| \end{aligned} \tag{4.17}$$

using the mean value theorem. Combining (4.8) with (4.12) and (4.17), we present the final regularity result for the Fourier coefficients $\hat{A}_n$:

$$\left|\hat{A}_n\right| \leq \frac{8\tau\sqrt{a}}{K'(l)\pi}\left(\frac{|v(0)|S_{max}}{(2n+1)^{3/2}} + \frac{3a\sup|v'(x)|}{\pi(2n+1)^2}\right). \tag{4.18}$$

Similarly, we define

$$\hat{B}_n = B_n \cosh\left(\frac{\pi n c}{a}\right), \tag{4.19}$$

so that

$$u(x+z_0) - \tau\left(1-\frac{x}{a}\right) = \sum_{n=1}^{\infty} \hat{B}_n \sin\left(\frac{\pi n x}{a}\right). \tag{4.20}$$

The coefficients $\hat{B}_n$ are given by

$$\begin{aligned}\hat{B}_n &= \frac{2}{a}\int_0^a \left(u(x+z_0) - \tau\left(1-\frac{x}{a}\right)\right)\sin\left(\frac{\pi n x}{a}\right)dx \\ &= \frac{2}{\pi n}\int_0^a \left(u_x(x+z_0) - \frac{\tau}{a}\right)\cos\left(\frac{\pi n x}{a}\right)dx \\ &= \frac{2\tau}{K'(l)\pi n}\operatorname{Im}\int_0^a \frac{v(x)}{\sqrt{x}}\cos\left(\frac{\pi n x}{a}\right)dx\end{aligned} \tag{4.21}$$

after applying integration by parts and dropping the constant slope term (the antiderivative of the cosine is the sine which vanishes on both endpoints). Using the same techniques as for $\hat{A}_n$ to evaluate the result, we get

$$\left|\hat{B}_n\right| \leq \frac{4\tau\sqrt{a}}{K'(l)\pi}\left(\frac{|v(0)|C_{max}}{\sqrt{2}n^{3/2}} + \frac{3a\sup|v'(x)|}{2\pi n^2}\right). \tag{4.22}$$

C_{max} is an upper bound of the absolute value of the Fresnel cosine integral. As per Lemma 4.3, we may use the value of the first local maximum $C_{max} = 0.779893$. [2, p. 329]

Lemma 4.3. *The Fresnel integral $S(x) = \int_0^x \cos\left(\frac{\pi}{2}t^2\right)dt$ is nonnegative for nonnegative real x, converges as $x \to \infty$, and the sequence of local maxima is decreasing monotonously.*

Proof. Using the substitution $z = t^2$, the Fresnel cosine integral may be rewritten as

$$S(x) = \frac{1}{2}\int_0^{x^2} \frac{\cos\left(\frac{\pi}{2}z\right)}{\sqrt{z}}dz.$$

The statments can be proved like in Lemma 4.2 using the Leibniz criterion. The only difference is that the first interval has only half the length as the other intervals, which makes an additional check necessary to show nonnegativity. Confirming that the first local minimum is positive [2, p. 329] concludes the proof. ∎

The regularity results agree well with the numerically measured $n^{-3/2}$ coefficient decay for large n.

We are not aware of a simple way to evaluate $\sup|v'(x)|$ (on the interval $[0,a]$) explicitly. However, we know that this function is analytic due to Lemma 4.1, which guarantees the existence of the supremum. It is computationally cheap to compute the extremal values of a well-behaving function like $v(x)$ using numerical methods.

4.2. Error bounds and convergence for coupled Laplace equations. As we have determined not only the shape of the coefficient decay, but also upper bounds for all involved constants, the results can be used to find an upper bound of the error of a numerically computed vector of N Fourier coefficients. Let A_n^∞ and B_n^∞ be the Fourier coefficients A_n and B_n of the exact solution. According to Lemma 2.2, A_n^∞ and B_n^∞ satisfy (2.5) and (2.4). Equations (2.13) and (2.12) can be corrected by adding the infinite sum remainders which were lost when using an $N \times N$ matrix only, such that they are exactly equivalent to (2.5) and (2.4). Define column vectors $\vec{\Delta}_A, \vec{\Delta}_B \in \mathbb{R}^N$:

$$\left(\vec{\Delta}_B\right)_i = \begin{cases} 0 & \text{if } i = 0 \\ -\frac{8}{\pi} \coth\left(\frac{\pi i c}{a}\right) \sum_{n=N}^{\infty} \frac{A_n^\infty \left(n+\frac{1}{2}\right)}{(2n+1)^2 - 4i^2} & \text{if } i \neq 0, \end{cases} \tag{4.23}$$

$$\left(\vec{\Delta}_A\right)_i = \frac{8}{\pi} \coth\left(\frac{\pi\left(i+\frac{1}{2}\right)b}{a}\right) \sum_{n=N}^{\infty} \frac{B_n^\infty n}{(2i+1)^2 - 4n^2}. \tag{4.24}$$

Denote with $\vec{A}_\infty\Big|_{\mathbb{R}^N}$ and $\vec{B}_\infty\Big|_{\mathbb{R}^N}$ the vectors containing the first N elements of A_∞ and B_∞, respectively. Correct (2.13) and (2.12) to

$$\vec{A}_\infty\Big|_{\mathbb{R}^N} = -\vec{v} + M_2 \vec{B}_\infty\Big|_{\mathbb{R}^N} + M_2 \vec{\Delta}_A, \tag{4.25}$$

$$\vec{B}_\infty\Big|_{\mathbb{R}^N} = M_1 \vec{A}_\infty\Big|_{\mathbb{R}^N} + M_1 \vec{\Delta}_B. \tag{4.26}$$

The coefficients with indices up to $N-1$ of A_n^∞ and B_n^∞ must be a solution of these equations. Solving for $\vec{A}_\infty\Big|_{\mathbb{R}^N}$, we may write

$$\vec{A}_\infty\Big|_{\mathbb{R}^N} = -\vec{v} + M_2 \left(M_1 \vec{A}_\infty\Big|_{\mathbb{R}^N} + M_1 \vec{\Delta}_B \right) + M_2 \vec{\Delta}_A. \tag{4.27}$$

According to Lemma 2.3, M is invertible, so the vector $\vec{A}^\infty$ of coefficients A_n^∞ with indices up to $N-1$ is the only solution.

$$\vec{A}_\infty\Big|_{\mathbb{R}^N} = M^{-1}\vec{v} - M^{-1}M_2M_1\vec{\Delta}_B - M^{-1}M_2\vec{\Delta}_A. \tag{4.28}$$

$$\|\vec{A}_\infty\Big|_{\mathbb{R}^N} - A^*\|_\infty \leq \|M^{-1}\vec{\Delta}_B\|_\infty + \|\vec{\Delta}_B\|_\infty + \|M^{-1}M_2\vec{\Delta}_A\|_\infty. \tag{4.29}$$

To investigate the order of convergence, first of all assume $|A_n| \leq C_A n^{-3/2}$ and $|B_n| \leq C_B n^{-3/2}$, where C_A and C_B are constants which can be determined using the results of the previous section. To find $\|\vec{\Delta}_B\|_\infty$, we approximate

$$\left|(\vec{\Delta}_B)_i\right| \leq \frac{2C_A}{\pi} \coth\left(\frac{\pi c}{a}\right) \sum_{n=N}^{\infty} \frac{1}{\sqrt{n}(n^2 - i^2)}. \tag{4.30}$$

We differentiate now between two cases. Without loss of generality, assume that N is even. If $i < N/2$, we can conclude that $\left|(\vec{\Delta}_B)_i\right| = \mathcal{O}(N^{-3/2})$ using the integral criterion. Otherwise, we evaluate the sum using the integral criterion to obtain [17]

$$\left|(\vec{\Delta}_B)_i\right| \leq \frac{C_A}{2\pi}\coth\left(\frac{\pi c}{a}\right)\left(\frac{\tanh^{-1}\left(\sqrt{\frac{i}{N}}\right)}{i^{3/2}} + \frac{4}{\sqrt{N}(N^2-i^2)}\right) = \mathcal{O}(N^{-3/2}\log(N)). \tag{4.31}$$

Together, this yields $\|\vec{\Delta}_B\|_\infty = \mathcal{O}(N^{-3/2}\log(N))$.

Lemma 4.4. *Let $T = I + S$, where S is the symmetric matrix defined in Lemma 2.3, such that $M = D^{-1}TD$. Then, $\|T^{-1}\|_{op} \leq 1$.*

Proof. Each eigenvector of S with eigenvalue η is also an eigenvector of T with eigenvalue $\lambda = \eta + 1$. Because S is positive semi-definite, $\eta \geq 0$ and thus $\lambda \geq 1$. T^{-1} has an eigenvalue $\lambda^{-1} \leq 1$. As S is symmetric, it is orthogonally diagonalizable as stated by the spectral theorem. Therefore

$$\|T^{-1}\|_{op} = \sup_{x\in\mathbb{R}^N}\frac{\|T^{-1}x\|}{\|x\|} = (\lambda^{-1})_{max} \leq 1.$$

■

We use Lemma 4.4 to estimate the remaining terms. We may write

$$\|M^{-1}\vec{\Delta}_B\|_\infty = \|D^{-1}T^{-1}D\vec{\Delta}_B\|_\infty \leq \|D\|_{op}\|T^{-1}\|_{op}\|D\vec{\Delta}_B\|_\infty = \mathcal{O}(N^{-1}\log(N)). \tag{4.32}$$

The last relation follows because the matrix multiplication with D results in another $\sqrt{i+1/2}$ term in the numerator of the expression for $\left|(\vec{\Delta}_B)_i\right|$. Similarly, we may write

$$\|M^{-1}M_2\vec{\Delta}_A\|_\infty \leq \|D\|_{op}\|T^{-1}\|_{op}\|DM_2\vec{\Delta}_A\|_\infty, \tag{4.33}$$

where

$$\left|(DM_2\vec{\Delta}_A)_i\right| \leq \frac{8\sqrt{2}C_B}{\pi^2}\coth\left(\frac{\pi b}{2a}\right)^2\sum_{j=1}^{N-1}\frac{j\sqrt{2i+1}}{|(2i+1)^2-4j^2|}\sum_{n=N}^{\infty}\frac{1}{\sqrt{n}(n^2-j^2)}. \tag{4.34}$$

$$\sum_{j=1}^{N/2-1}\frac{j\sqrt{2i+1}}{|(2i+1)^2-4j^2|}\sum_{n=N}^{\infty}\frac{1}{\sqrt{n}(n^2-j^2)} \leq \frac{\mathcal{O}(1)}{N^{3/2}}\sqrt{2i+1}\sum_{j=1}^{N/2-1}\frac{j}{|4j^2-(2i+1)^2|}. \tag{4.35}$$

The given series over j can be decomposed into two different series ($j > i$ and $j \leq i$) to account for the absolute value function. These can be further decomposed into a total of four series by utilizing the partial fraction decomposition

$$\frac{j}{4j^2-(2i+1)^2} = \frac{1}{4(2j+2i+1)} + \frac{1}{4(2j-2i-1)}. \tag{4.36}$$

Each of these four series contains at most $N/2$ elements. The expressions $2j+2i+1$ and $2j-2i-1$ are linear in j, therefore, the elements in each series are distinct odd numbers. This shows that the original series has an upper bound of four times the harmonic series with $N/2$ elements. Given that i is bounded by N, $\left|(DM_2\vec{\Delta}_A)_i\right| \leq \mathcal{O}(N^{-1}\log(N))$. The same

computation can be performed for the case $j > N/2 - 1$ using equation (4.31), which yields $\left|(DM_2\vec{\Delta}_A)_i\right| \leq \mathcal{O}(N^{-1}\log^2(N))$. Combining the results from this section, we may conclude

$$\|\vec{A}_\infty\Big|_{\mathbb{R}^N} - A^*\|_\infty = \mathcal{O}(N^{-1}\log^2(N)). \tag{4.37}$$

It should be noted that it is also possible to compute explicit error bounds (not only the order of convergence). They have been omitted in this paper for the sake of brevity. Furthermore, it is possible to plug in numerical values to compute the error bounds of a specific computation, which may lead to a lower actual error compared to the estimates performed in this section (this would, for example, be the case for a nearly-diagonal matrix M, which would be expected if the parameters a, b, c are of the same order of magnitude). In contrast to alternative methods like investigating the stability of the convergence of a computed value as $N \to \infty$, this method provides a guarantee that the exact solution must be within the error bounds of the numerically computed solution.

5. Experimental results.

The 2D geometry investigated above can be extended along the z-axis to receive a 3D geometry which can be constructed by placing a strip of an aluminium sheet between two thermally insulating XPS plates (as shown in Figure 5). The aluminium is heated on one side and cooled on the other. Five temperature sensors are placed on the aluminium strips at different positions z. The measured equilibrium temperature values (for $a = (21.0 \pm 0.5)\,\text{mm}$, $b = (12.5 \pm 0.5)\,\text{mm}$ and $c = (7.5 \pm 0.5)\,\text{mm}$) are shown in Table 1. The last column denotes the temperature difference to the ambient temperature of $(26.5 \pm 1.0)\,\text{C}$.

Under the assumption that the thermal conductivity of the XPS foam $\lambda_{XPS} = 0$, there is only heat flow in the z-direction, which implies that the temperature inside the aluminium strip $\tau(z)$ is a linear function of z. For $\lambda_{XPS} > 0$, however, heat is lost along the x- and y-axes. It will be shown below that in this case, $\tau(z)$ is not linear and has a curvature depending on the coefficient β computed in the previous sections.

Table 1: Measured temperature values

Sensor	**Position z (cm)**	**Temperature (°C)**	**τ (K)**
A	0.0	75.4	48.9
B	4.0	59.1	32.6
C	7.0	49.9	23.4
D	12.5	36.4	9.9
E	15.0	30.9	4.4

The following simplifications are made:

- The thickness of the aluminium strip along the x-axis is negligible.
- The length of the setup along the z-axis is long enough such that the heat flowing through the XPS foam boundary areas parallel to the xy-plane is negligible.
- The XPS foam boundary areas parallel to the xz- and yz-planes have the same temperature as the ambient air (in other words, the heat transfer coefficient between XPS foam and air is large).

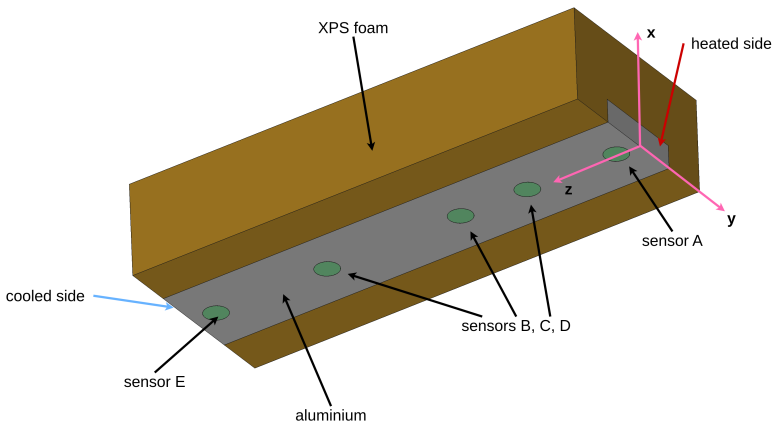

Figure 5: 3D sketch of the experimental setup (not to scale, and temperature sensor positions are arbitrary). Only the upper part ($x \geq 0$) is shown for better understanding, exploiting symmetry with respect to the yz-plane.

The heat equation applied along the z-direction is:

$$P(z) = -\lambda_{Al}(2c)d\frac{d\tau(z)}{dz}, \tag{5.1}$$

where $d = (0.50 \pm 0.05)\,\mathrm{mm}$ is the thickness of the aluminium strip. Equation (2.20) may be rewritten to:

$$\frac{dP(z)}{dz} = -4\beta\lambda_{XPS}\tau(z). \tag{5.2}$$

Here is also considered that the previous calculations investigated only one quarter of the system. Taking the derivative of (5.1) and combining with (5.2):

$$-\lambda_{Al}cd\frac{d^2\tau(z)}{dz^2} = -2\beta\lambda_{XPS}\tau(z). \tag{5.3}$$

The general solution of this differential equation is

$$\tau(z) = A\sinh(\mu z) + B\cosh(\mu z), \tag{5.4}$$

where

$$\mu = \sqrt{\frac{2\beta\lambda_{XPS}}{\lambda_{Al}cd}}, \tag{5.5}$$

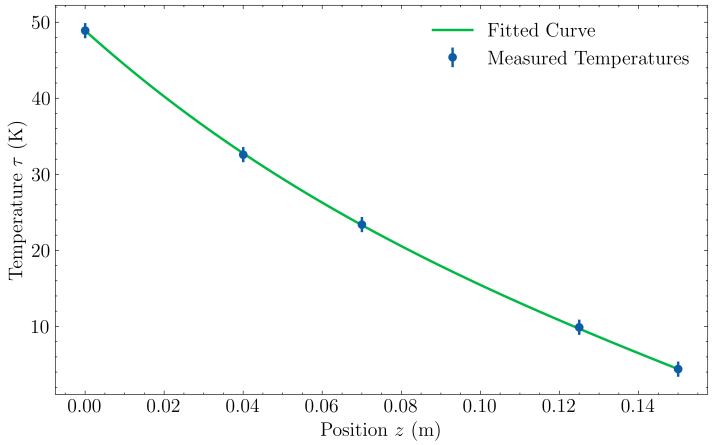

Figure 6: Experimentally measured temperature τ (the difference between the core temperature in the aluminium strip and the ambient temperature) in terms of the position z for a 3D version of the rectangular cross section investigated in this paper

$$B = \tau_A. \tag{5.6}$$

Define $H = z_E - z_A = 15.0cm$.

$$A = \frac{\tau_E - \tau_A \cosh(\mu H)}{\sinh(\mu H)}. \tag{5.7}$$

The available values for the thermal conductivities of commercially used Aluminium (which does not have 100% purity) and XPS vary [4, 1, 6, 7, 12, 11]. Here we use $\lambda_{Al} = (215 \pm 10)\,\mathrm{Wm^{-1}K^{-1}}$ and $\lambda_{XPS} = (0.035 \pm 0.005)\,\mathrm{Wm^{-1}K^{-1}}$.

Fitting the measured values from table Table 1 to formula (5.4) with the computed constants, as shown in Figure 6 yields $\mu = (8.60 \pm 0.14)\,\mathrm{m^{-1}}$. Formula (5.5) gives $\beta = 0.85 \pm 0.17$, which is in good agreement with the computed value $\beta = 0.890$ from equation (3.13). The fitted value of μ has a low statistical error, most inaccuracies of the measured value of β come from uncertainties in the properties of the materials used as well as systematic errors (the temperature of the XPS surface is actually not equal to the ambient temperature, and heat flux through XPS perpendicular to the cross section is ignored in our model).

6. Conclusions. We solve a Laplace equation with a 180 degree Dirichlet-Neumann boundary type transition via two different methods.

By cutting the domain into two parts along the horizontal line through the point of the boundary type transition, we are left with two parts having both Dirichlet and Neumann conditions on the sides of the rectangle, but never two different conditions on different segments of the same side of the rectangle. We find the general solution of the Laplace equation in each part using separation of variables. This computation yields a sequence of Fourier coefficients which must be determined by applying the additional conditions of continuity of the temperature and its derivative along the domain cut. The exact solution requires the inversion of an infinite matrix, but it can be well approximated by only considering a finite

number of Fourier coefficients. The resulting temperature field is shown in Figure 3. The geometrical heat flux coefficient β as defined in (2.20) can be retrieved using equation (2.21).

Alternatively, the problem can be solved by creating a conformal mapping - consisting of an inverse Christoffel-Schwarz transformation, a Möbius transformation and a Christoffel-Schwarz transformation - between the original domain and another rectangle where the solution is easy to obtain (a linear function of the vertical coordinate / imaginary part). As the Laplace equation is invariant under conformal mappings, we may transform this solution back into the original domain. As expected, the temperature field retrieved by this method looks visually the same as for the coupled solution. The formula for β is (3.13), which is equal to the value of β that would be found for the linear solution in the transformed domain (the aspect ratio of the rectangle).

Our regularity results show that the Fourier coefficients are decaying like $n^{-3/2}$ for large n, which is due to a square root singularity at the boundary condition type transition point. Additionally, we prove formulas for explicit upper bounds of the absolute values of the coefficients. These equations include the supremum of an analytic function on a compact interval, which must be computed numerically. The regularity results allow one to determine an upper bound for the maximum error of a solution computed considering only a finite number of Fourier coefficients.

We conducted an experiment consisting of a 3D object having the cross-section investigated in this paper. Experimental results agree well with the theory. The strongest source of errors is the inaccuracy of available values for properties of the used materials, like the thermal conductivity of the XPS used, or the thickness of the aluminium sheet.

Acknowledgments. Many thanks to project advisor Prof. Dr. Giovanni Felder for his support, and to everybody else who provided hints.

REFERENCES

[1] AALCO, *Aluminium alloy - commercial alloy - 1050a h14 sheet*, Jan. 2023, https://www.aalco.co.uk/datasheets/Aluminium-Alloy-1050A-H14-Sheet_57.ashx.

[2] M. ABRAMOWITZ AND I. A. STEGUN, *Handbook of Mathematical Functions with Formulas, Graphs, and Mathematical Tables*, Dover Publications, 10th ed., Dec 1972.

[3] S. AXLER, P. BOURDON, AND W. RAMEY, *Harmonic Function Theory*, Springer New York, 2001, https://doi.org/10.1007/978-1-4757-8137-3.

[4] AZO MATERIALS, *Aluminium - the resource*, Apr. 2001, https://www.azom.com/properties.aspx?ArticleID=309.

[5] G. BARTON AND G. BARTON, *Elements of Green's Functions and Propagation: Potentials, Diffusion, and Waves*, Oxford science publications, Clarendon Press, 1989, https://books.google.ch/books?id=-iPwVGfDtecC.

[6] BATZ BURGEL, *Aluminum semi-finished en aw-1050a*, Jan. 2023, https://batz-burgel.com/en/metal-trading/aluminium-product-range/en-aw-1050/.

[7] C-THERM TECHNOLOGIES LTD., *Thermal conductivity of xps (extruded polystyrene) foam*, Feb. 2020, https://ctherm.com/resources/newsroom/blog/thermal-conductivity-xps-extruded-polystyrene-foam/.

[8] W. P. CALIXTO, B. ALVARENGA, J. C. DA MOTA, L. D. C. BRITO, M. WU, A. J. ALVES, L. M. NETO, AND C. F. R. L. ANTUNES, *Electromagnetic problems solving by conformal mapping: A mathematical operator for optimization*, Mathematical Problems in Engineering, 2010 (2010), pp. 1–19, https://doi.org/10.1155/2010/742039.

[9] H. E. Haber, *Uniqueness of solutions to the laplace and poisson equations*, 2012, http://scipp.ucsc.edu/~haber/ph116C/Laplace_12.pdf.

[10] M. Iacobelli, *Notes analysis 3 - eth zurich*, Jan. 2022, https://metaphor.ethz.ch/x/2021/hs/401-0353-00L/lec/A3_LC.pdf.

[11] Kingspan, *Types of insulation - a guide*, Apr. 2024, https://www.kingspan.com/gb/en/knowledge-articles/types-of-insulation-a-guide/.

[12] Nuclear Power, *Extruded polystyrene – xps*, Jan. 2023, https://www.nuclear-power.com/nuclear-engineering/heat-transfer/heat-losses/insulation-materials/extruded-polystyrene-xps/.

[13] K. A. Ott and R. M. Brown, *The mixed problem for the laplacian in lipschitz domains*, Potential Analysis, 38 (2012), pp. 1333–1364, https://doi.org/10.1007/s11118-012-9317-6.

[14] A. Peirce, *Lecture 25: More rectangular domains: Neumann problems, mixed bc, and semi-infinite strip problems*, Aug. 2017, https://personal.math.ubc.ca/~peirce/M257_316_2012_Lecture_25.pdf.

[15] H. M. Srivastava, K. Y. Kung, and K. J. Wang, *Analytic solutions of a two-dimensional rectangular heat equation*, Russian Journal of Mathematical Physics, 14 (2007), pp. 115–119, https://doi.org/10.1134/s1061920807010086.

[16] user98130 (https://math.stackexchange.com/users/98130/user98130), *Linear transformations mapping four points*. Mathematics Stack Exchange, https://math.stackexchange.com/q/512913.

[17] Wolfram Research, Inc., *Mathematica, Version 13.0.1.0*, https://www.wolfram.com/mathematica. Champaign, IL, 2022.